Contrib Mineral Petrol (2011) 161:213–227
DOI 10.1007/s00410-010-0527-x

ORIGINAL PAPER

Ternary Ca–Fe–Mg carbonates: subsolidus phase relations at 3.5 GPa and a thermodynamic solid solution model including order/disorder

E. Franzolin · M. W. Schmidt · S. Poli

Received: 4 December 2009 / Accepted: 6 April 2010 / Published online: 22 April 2010
© Springer-Verlag 2010

Abstract Subduction carries atmospheric and crustal carbon hosted in the altered oceanic crystalline basement and in pelagic sediments back into the mantle. Reactions involving complex carbonate solid solutions(s) lead to the transfer of carbon into the mantle, where it may be stored as graphite/diamond, in fluids or melts, or in carbonates. To constrain the thermodynamics and thus reactions of the ternary Ca–Mg–Fe carbonate solid solution, piston cylinder experiments have been performed in the system $CaCO_3$–$MgCO_3$–$FeCO_3$ at a pressure of 3.5 GPa and temperatures of 900–1,100°C. At 900°C, the system has two miscibility gaps: the solvus dolomite–calcite, which closes at X_{MgCO3} ~0.7, and the solvus dolomite–magnesite, which ranges from the Mg to the Fe side of the ternary. With increasing temperature, the two miscibility gaps become narrower until complete solid solutions between $CaCO_3$–$Ca_{0.5}Mg_{0.5}CO_3$ is reached at 1,100°C and between $CaCO_3$–$FeCO_3$ at 1,000°C. The solvi are characterized by strong compositional asymmetry and by an order–disorder mechanism. To deal with these features, a solid solution model based on the van Laar macroscopic formalism has been calculated for ternary carbonates. This thermodynamic solid solution model is able to reproduce the experimentally constrained phase relations in the system $CaCO_3$–$MgCO_3$–$FeCO_3$ in a broad P–T range. To test our model, calculated phase equilibria were compared with experiments performed in carbonated mafic protolithes, demonstrating the reliability of our solid solution model at pressures up to 6 GPa in complex systems.

Keywords Carbonates · Mantle · Subduction · Thermodynamic · Solid solution

Communicated by T. L. Grove.

E. Franzolin (✉) · M. W. Schmidt
Institute of Geochemistry and Petrology,
ETH, 8092 Zurich, Switzerland
e-mail: ettore.franzolin@erdw.ethz.ch

S. Poli
Dipartimento di Scienze della Terra,
Universita' degli Studi di Milano,
20133 Milan, Italy

Introduction

At convergent margins, volatile components are recycled into the mantle. CO_2 is fixed in the form of carbonates in oceanic sediments, mafic oceanic crust and to a lesser extent in sub MOR peridotite during hydrothermal alteration (Staudigel 2003). Upon subduction, carbonates are generally more refractory than hydrous phases, and fluids are H_2O dominated (Molina and Poli 2000; Connolly 2005; Poli et al. 2009). Therefore, CO_2 remains preferentially in the slab (Kerrick and Connolly 2001) and is carried beyond subarc depths down into the mantle. Findings of carbonate-bearing UHP mineral assemblages represent natural evidence of the stability of carbonates at upper mantle pressures. Inclusions of magnesite in natural diamonds from the Finsch kimberlite pipe in South Africa (Wang et al. 1996) demonstrate the occurrence of carbonates in the mantle at depths exceeding 120 km. Similar dolomite and Ba–Sr carbonate inclusions in diamonds, from two different kimberlite regions of the Siberian craton, have been reported by Logvinova et al. (2008). Carbonate–diamond parageneses have been discovered not only in a sub-cratonic geodynamic context, but also as subduction-related: the formation of microdiamonds associated with (Ba,Ca,Mg)CO_3, magnesite and dolomite has been documented by van Roermund

et al. (2002) in a mantle-derived peridotite lens from Bardane, Fjørtoft, western Norway. Moreover, Korsakov and Hermann (2006) described subducted carbonated sediments from the Kokchetav massif containing inclusions of magnesian calcite intergrowing with micro-diamonds in garnet and clinopyroxene. Mukherjee et al. (2003) reported the finding of UHP carbonate-bearing coesite eclogites of subducted Indian continental crust containing dolomite, magnesite and Mg calcite with significant amounts of FeO. These natural occurrences of carbonates at UHP conditions document that carbonate compositions span from Fe-bearing magnesite to dolomite-ankerite$_{s.s.}$ to Mg–Fe calcite.

Despite the main role of carbonates in cycling back atmospheric CO_2 into the mantle, few experimental data are available to thermodynamically model the behavior of this mineral group at high pressure. Thus, this study defines the phase relations of the ternary carbonate system at 3.5 GPa, filling a decisive gap for deriving thermodynamic properties valid at high pressures. We then fit a ternary solid solution model to the entity of the existing experimental data. The solid solution model, based on data from 0.2 to 6 GPa, then allows computing high pressure phase equilibria in CO_2-bearing systems, for which two examples are presented to pressures of 6 GPa.

The experimental background on the occurrence of carbonates at high pressure

Previous experimental studies demonstrate that the composition of carbonates is very dependent on pressure and bulk composition (Dasgupta et al. 2005). In subducted mafic crust, calcite is generally stable at lower pressure than dolomite, whereas magnesite is stable above 4–5 GPa (Dasgupta et al. 2004). In carbonated pelites, dolomite or Mg–Fe calcite is stable at relatively lower pressures (Thomsen and Schmidt 2008a, b), but magnesite is the only CO_2-bearing mineral present at depths greater than 180 km (Domanik and Holloway 2000). Experiments carried out in ultramafic systems reveal that with increasing pressure, dolomite and ultimately magnesite are stable at upper mantle conditions (Brey et al. 2008; Dasgupta and Hirschmann 2007; Dasgupta et al. 2007; Falloon and Green 1989). Experiments performed on pelitic and mafic eclogites show that an Fe-bearing intermediate term of the solid solution dolomite–calcite is stable to pressures of at least 5 GPa (Dasgupta et al. 2004; Thomsen and Schmidt 2008b; Yaxley and Brey 2004). The influence of Fe on the stability and structure of this carbonate is largely unknown, this phase being described as Cc-Dol$_{s.s.}$ (Dasgupta et al. 2004; Yaxley and Brey 2004), Mg–Fe calcite (Thomsen and Schmidt 2008b), calcite or dolomite (Hammouda 2003) without any structural information. The stability field of Mg–Fe calcite is bulk composition dependent: for starting materials having $X_{Ca} > 0.4$, Mg–Fe calcite is stable up to 6 GPa (Yaxley and Brey 2004), whereas for more magnesian bulk compositions, i.e., peridotitic systems ($X_{Ca} = 0.05$) magnesite is already stable at pressure as low as 4 GPa (Dasgupta and Hirschmann 2006).

Magnesite is also the product of the reaction dolomite = magnesite + aragonite. This reaction, which occurs at pressures above 5 GPa and temperatures between 600 and 1,000°C, was experimentally determined in several laboratories leading to diverging results in the location and curvature of this reaction (Buob et al. 2006; Luth 2001; Martinez et al. 1996; Sato and Katsura 2001; Shirasaka et al. 2002). Diamond-anvil experiments demonstrate that magnesite is the only stable carbonate in the lower mantle (Biellmann et al. 1993; Gillet 1993) and in situ X-ray diffraction study suggests that $MgCO_3$ is stable in a hitherto undetermined structure down to the core–mantle boundary (Isshiki et al. 2004). Also, $CaCO_3$ is stable up to >130 GPa (Ono et al. 2007) and dolomite to >9 GPa (Luth 2001), persisting at room temperature metastably to >28 GPa (Kraft et al. 1991). Nevertheless, because magnesite is the more stable carbonate at pressure beyond 4 GPa in peridotitic systems (Dasgupta and Hirschmann 2006), it is allegedly the only carbonate in the deep mantle.

Even though the stability of carbonates in the mantle has been observed in natural samples and confirmed by experimental work in simple and more complex systems, few thermodynamic constraints are available for ternary Ca–Mg–Fe carbonates at high pressure. The combination of natural data and experimental phase relations in $CaCO_3$–$MgCO_3$–$FeCO_3$ and in $CaCO_3$–$MgCO_3$ have been combined to model ternary carbonates (Anovitz and Essene 1987; Davidson 1994; Mcswiggen 1993a, b). However, these solid solution models have two main flaws: they are both not reliable at high pressure and they are not easily implementable into a practical thermodynamic formalism. Therefore, it is current practice in phase equilibria calculations to treat ternary carbonates using two distinct binary solid solution models: dolomite-ankerite and magnesite-siderite (Kerrick and Connolly 2001). This approach fails to describe the role of Ca in the ternary solid solution and it is not able to predict the stability of Mg–Fe calcite.

Previous experimental data and thermodynamic modeling in the system $CaCO_3$–$MgCO_3$–$FeCO_3$

The system $CaCO_3$–$MgCO_3$ has been extensively investigated at various pressures up to 6 GPa (Buob et al. 2006; Irving and Wyllie 1975), though few experimental data are available on the system $CaCO_3$–$FeCO_3$ (Davidson et al. 1993; Rosenberg 1963). The first experimental study

describing phase relations in the system $CaCO_3$–$MgCO_3$–$FeCO_3$ was conducted by Goldsmith et al. (1962), who determined isothermal sections at temperatures between 600 and 800°C at 1.5 GPa (Fig. 1b, c). At temperatures above 650°C, Goldsmith et al. (1962) demonstrate the presence of two 2-phase fields (black dots in Fig. 1), where dolomite coexists with calcite or magnesite, resembling the phase relations of the system $CaCO_3$–$MgCO_3$ (Goldsmith and Heard 1961). With increasing Fe content, the miscibility gap dolomite-calcite narrows until it closes at X_{CaCO3} ~0.7 and X_{MgCO3} ~0.1 between 700 and 800°C. The second 2-phase field is a broad dolomite-magnesite miscibility gap that extends from the Mg to the Fe side, where siderite coexists with $Ca_{0.7}Fe_{0.3}CO_3$ at 700°C and with $Ca_{0.6}Fe_{0.4}CO_3$ at 800°C. Furthermore, at temperature below 700°C, Goldsmith et al. (1962) obtained coexistence of Fe dolomite, Fe calcite and Mg siderite defining a three-phase field (Fig. 1b), which broadens with decreasing temperature.

The experiments by Rosenberg (1967) were run at 0.2–0.3 GPa and 350–550°C (Fig. 1a) and confirmed the presence of a three phase field as observed by Goldsmith et al. (1962). Increasing the temperature from 400 to 500°C, the three phase field moves toward the join $CaCO_3$–$FeCO_3$ (Fig. 1a). The discrepancy between the three phase fields determined by Goldsmith et al. (1962) and by Rosenberg (1967) can be attributed to differences in pressure and temperature, or to uncertainties in the experimental and analytical techniques. Indeed, neither experimental work has performed textural analysis of the quenched experimental charges. Instead, the mineralogical composition of the run products was determined by X-ray powder diffraction, leading to average compositions of synthesized phases calculated from cell parameters. Furthermore, these experiments were very short: less than 1 day for the experiments performed by Goldsmith et al. (1962) and 2 days for those of Rosenberg (1967) at 550°C.

Carbonates are characterized by complex solid solution relations dominated by interactions among a disordered "calcite-like" structure $R\bar{3}c$ and an ordered "dolomite-like" structure $R\bar{3}$. Solid solution models that describe the binary system $CaCO_3$–$MgCO_3$ have been proposed by Burton and Kikuchi (1984), Burton (1987), Holland and Powell (2003), Vinograd et al. (2007), and Vinograd et al. (2006). Davidson et al. (1993) and Vinograd et al. (2006) have introduced models for the system $CaCO_3$–$FeCO_3$. Solid solution models for the ternary system $CaCO_3$–$MgCO_3$–$FeCO_3$ have been proposed by Anovitz and Essene (1987), Davidson (1994), and McSwiggen (1993a, b).

The solid solution model of Anovitz and Essene (1987) was based on the analysis of natural carbonates with formation temperatures between 250 and 700°C. It uses a subregular formalism and two sets of independent mixing parameters to describe energy interactions within disordered structures separately from ordered structures; the ordering state is therefore implicit. As suggested by Anovitz and Essene, their model should not be used at temperatures above 800°C; therefore, the major weakness of this model is the incapability to reproduce critical conditions at which solvi between ordered and disordered phases close (i.e., between dolomite and calcite or magnesite).

McSwiggen (1993a, b) combined a Bragg–Williams model, which describes the state of order as a function of temperature and composition, with a Margules interaction model based on experimental data available for the binary join $CaCO_3$–$MgCO_3$ and $CaCO_3$–$FeCO_3$. The ternary solvi are then constrained both by natural and experimental data. The result is a very complex model employing 52 solid solution parameters. This model is able to predict phase relations in the ternary system to a temperature of 700°C, but has been ignored and gone unapplied because of its complexity.

The most recent model for the $CaCO_3$–$MgCO_3$–$FeCO_3$ ternary by Davidson (1994) is based on the ternary extension of the "General Point Approximation model" (Capobianco et al. 1987). The phase diagram calculated predicts complete solid solution between dolomite and ankerite ($CaFe(CO_3)_2$) at 530°C, in disagreement with previous experimental data (Goldsmith et al. 1962; Rosenberg 1967) and with experiments performed in the system $CaCO_3$–$FeCO_3$, which have not demonstrated the stability of ordered ankerite (Davidson et al. 1993).

The solid solution model we present in this study is based on new experimental data performed at 3.5 GPa in the ternary system $CaCO_3$–$MgCO_3$–$FeCO_3$. We incorporate the degree of order in the solid solution introducing two order compounds. Activity–composition relations are expressed according to the van Laar formulation (Holland and Powell 2003), which allows describing asymmetrical miscibility gaps.

Experimental and analytical methods

The starting materials consist of mixtures of pure synthetic calcite, pure natural magnesite from Obersdorf (Philipp 1998) and synthetic siderite. Siderite has been multiply synthesized in externally heated cold seal vessels at 200 MPa and 350°C from iron oxalate sealed into gold capsules of 5.4 mm O.D. following French (1971). The starting materials were ground; calcite and magnesite were dried at 220°C for ≥16 h, and stored at 110°C. Siderite was stored at ambient temperature in a desiccator to slow its nevertheless unavoidable oxidation.

All experiments (Table 1) were run at ETH, Zurich in end-loaded piston cylinders with assemblies made of

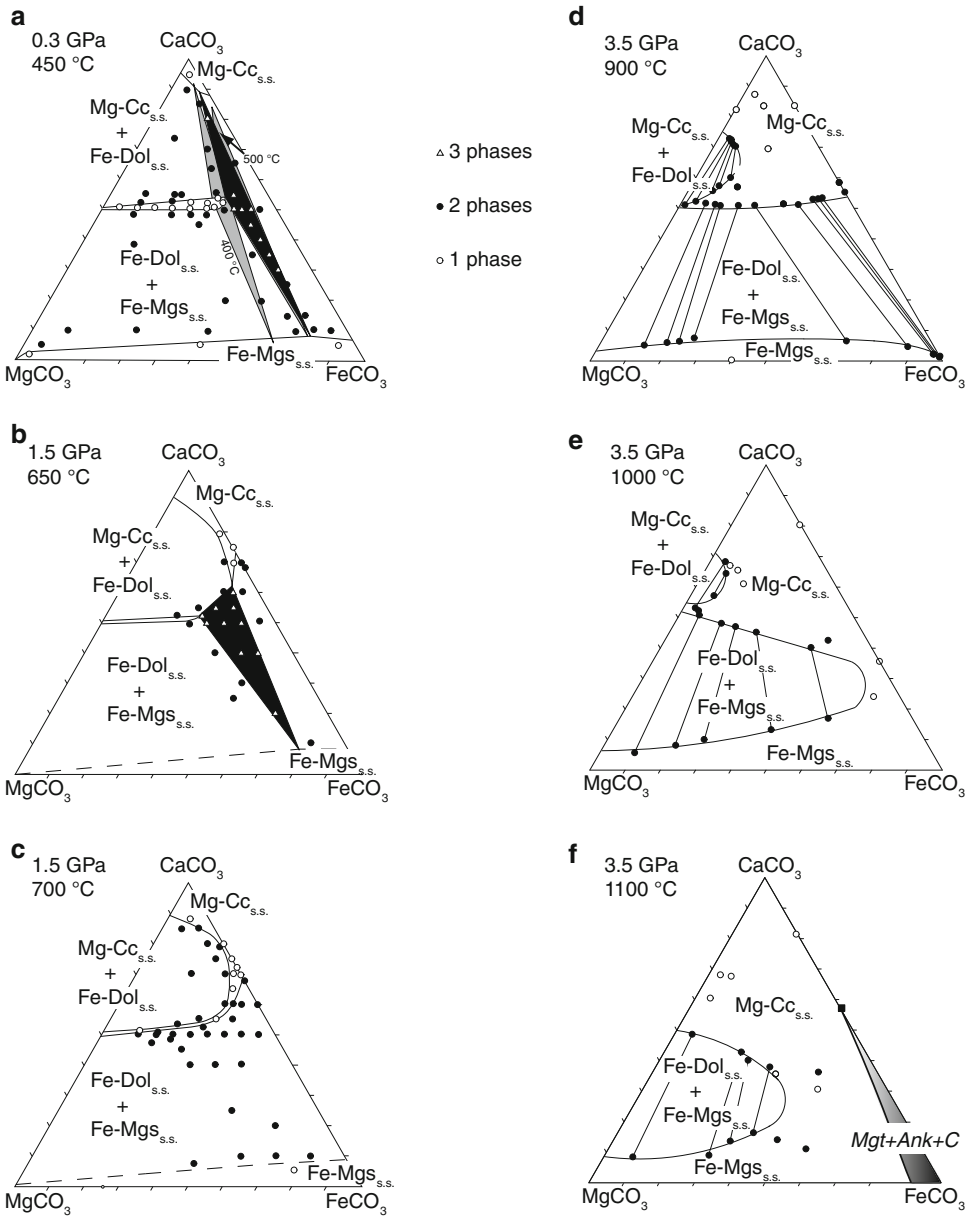

Fig. 1 Summary of the known subsolidus phase relations in the pseudo-ternary system $CaCO_3$–$MgCO_3$–$FeCO_3$ including our new results (*right hand side*). **a**, **b**, **c** *Open circles* indicate single phase, *filled circles* two phase, and *open triangles* three phase run products. The *symbols* in **a**–**c** give bulk compositions of the starting material and not compositions of the (unmeasured) synthesized phases. **a** 0.3 GPa, 450°C, after Rosenberg (1967). The *filled black triangle* delineates the three phase field at 450°C, the *gray triangles* indicate those at 400 and 500°C. **b**, **c** 1.5 GPa, 650 and 700°C, after Goldsmith et al. (1962). The *filled black triangle* in **b** shows the three phase field, such a field appears to be absent at 700°C. **d**, **e**, **f** 3.5 GPa, 900, 1,000, and 1,100°C, this study. Unlike in **a**–**c**, *circles* represent measured compositions of phases synthesized in the experiments summarized in Table 1; coexisting phases are joined with tie-lines. **f** *Black square* ankeritic carbonate resulting from the redox break-down of more Fe-rich carbonates to $ankerite_{ss}$ + magnetite + graphite according to Eq. 1. *Shadowed area* field where carbonates in this pseudo-ternary are unstable due to redox reaction (1). All phase boundaries represent a visual fit to the data

NaCl–Pyrex–salt–MgO. To avoid major siderite oxidation, experiments were run with inner graphite capsules placed in a welded 4.6 mm O.D. Pt capsule. Temperature was controlled by Eurotherm controllers within ±2°C, using B-type ($Pt_{94}Rh_6/Pt_{70}Rh_{30}$) thermocouples; quenching was done by turning off power to the furnace.

Capsules were embedded in epoxy and ground to expose phase assemblages, which have been analyzed with a JEOL JXA8200 electron microprobe at ETH using 15 kV acceleration voltage. Textural relationships between phases were studied using backscattered electron (BSE) imaging. To avoid volatilization of carbonates under the electron

Table 1 Run conditions and run products of the experiments

Run	Starting material (wt%)			T	Run Products	Phase 1 (mol.%)			Phase 2 (mol.%)		
	Cc	Mgs	Sid	(°C)		Cc	Mgs	Sid	Cc	Mgs	Sid
b.c a	50	0	50	900	$(Ca,Fe)CO_3$	0.58	0.00	0.41	–	–	–
b.c b	40	20	40	900	$(Ca,Mg,Fe)CO_3$	0.49	0.21	0.30	–	–	–
b.c c	50	25	25	900	$(Ca,Mg,Fe)CO_3$	0.57	0.30	0.13	–	–	–
b.c d	18.5	44.5	37	900	$Dol_{s.s.} + Mgs_{s.s}$	0.51	0.32	0.17	0.07	0.67	0.26
b.c e	30	10	60	900	$Dol_{s.s.} + Mgs_{s.s.}$	0.51	0.12	0.36	0.02	0.01	0.96
b.c f	65	10	25	900	$(Ca,Mg,Fe)CO_3$	0.70	0.15	0.16	–	–	–
b.c g	30	60	10	900	$Dol_{s.s.} + Mgs_{s.s}$	0.52	0.41	0.07	0.05	0.82	0.12
b.c i	20	5	75	900	$Dol_{s.s.} + Mgs_{s.s}$	0.51	0.08	0.42	0.03	0.02	0.98
b.c l	80	10	10	900	$(Ca,Mg,Fe)CO_3$	0.84	0.09	0.08	–	–	–
b.c m	85	10	5	900	$(Ca,Mg,Fe)CO_3$	0.87	0.10	0.03	–	–	–
b.c n	70	25	5	900	$Cc_{s.s.} + Dol_{s.s.}$	0.73	0.24	0.03	0.51	0.48	0.01
b.c o	60	35	5	900	$Cc_{s.s.} + Dol_{s.s.}$	0.72	0.24	0.04	0.52	0.44	0.04
b.c q	25	25	50	900	$Dol_{s.s.} + Mgs_{s.s}$	0.51	0.28	0.21	0.07	0.24	0.69
b.c r	25	10	65	900	$Dol_{s.s.} + Mgs_{s.s}$	0.51	0.15	0.33	0.05	0.07	0.88
b.c s	25	0	75	900	$Dol_{s.s.} + Mgs_{s.s}$	0.53	0.00	0.47	0.02	0.00	0.98
b.c t	75	0	25	900	$(Ca,Fe)CO_3$	0.84	0.00	0.16	–	–	–
b.c k	10	30	60	900	$Dol_{s.s.} + Mgs_{s.s.}$	0.51	0.39	0.10	0.06	0.75	0.19
b.c j	0	40	60	900	$(Mg,Fe)CO_3$	0.00	0.60	0.40	–	–	–
b.c w	35	5	60	900	$Dol_{s.s.} + Mgs_{s.s}$	0.50	0.09	0.42	0.02	0.01	0.97
b.c z	56	24	20	900	$Cc_{s.s.} + Dol_{s.s.}$	0.70	0.24	0.06	0.60	0.30	0.10
b.c x	60	25	15	900	$Cc_{s.s.} + Dol_{s.s.}$	0.71	0.24	0.05	0.57	0.35	0.08
b.c y	63	27	10	900	$Cc_{s.s.} + Dol_{s.s.}$	0.72	0.24	0.04	0.56	0.37	0.07
b.cAD	12.5	37.5	50	900	$Dol_{s.s.} + Mgs_{s.s.}$	0.51	0.38	0.12	0.07	0.71	0.22
b.cAF	90	10	0	900	$(Ca,Mg,Fe)CO_3$	0.82	0.18	0.00	–	–	–
b.c e	30	10	60	1,000	$(Ca,Mg,Fe)CO_3$	0.43	0.11	0.46	–	–	–
b.c g	30	60	10	1,000	$Dol_{s.s.} + Mgs_{s.s}$	0.51	0.44	0.06	0.06	0.84	0.10
b.c h	65	25	10	1,000	$Cc_{s.s.} + Dol_{s.s.}$	0.67	0.27	0.06	0.54	0.39	0.07
b.c i	20	5	75	1,000	$(Ca,Mg,Fe)CO_3$	0.24	0.07	0.68	–	–	–
b.c n	70	25	5	1,000	$Cc_{s.s.} + Dol_{s.s.}$	0.68	0.27	0.04	0.53	0.43	0.03
b.c o	60	35	5	1,000	$(Ca,Mg,Fe)CO_3$	0.52	0.43	0.05	–	–	–
b.c p	25	37.5	37.5	1,000	$Dol_{s.s.} + Mgs_{s.s}$	0.48	0.39	0.13	0.08	0.71	0.20
b.c s	25	0	75	1,000	$(Ca,Fe)CO_3$	0.36	0.00	0.64	–	–	–
b.c t	75	0	25	1,000	$(Ca,Fe)CO_3$	0.80	0.00	0.20	–	–	–
b.c z	56	24	20	1,000	$(Ca,Mg,Fe)CO_3$	0.61	0.26	0.13	–	–	–
b.c x	60	25	15	1,000	$(Ca,Mg,Fe)CO_3$	0.65	0.25	0.09	–	–	–
b.c y	63	27	10	1,000	$(Ca,Mg,Fe)CO_3$	0.66	0.27	0.07	–	–	–
b.cAG	25.6	38.8	35.6	1,000	$Dol_{s.s.} + Mgs_{s.s}$	0.47	0.35	0.18	0.10	0.63	0.27
b.cAH	24.4	24.7	50.9	1,000	$Dol_{s.s.} + Mgs_{s.s}$	0.44	0.26	0.30	0.13	0.42	0.45
b.cAI	23.35	11.8	64.85	1,000	$Dol_{s.s.} + Mgs_{s.s}$	0.40	0.17	0.43	0.17	0.24	0.59
b.c d	18.5	44.5	37	1,100	$Dol_{s.s.} + Mgs_{s.s}$	0.43	0.35	0.22	0.09	0.61	0.29
b.c e	30	10	60	1,100	$(Ca,Mg,Fe)CO_3$	0.36	0.17	0.47	–	–	–
b.c g	30	60	10	1,100	$Dol_{s.s.} + Mgs_{s.s}$	0.49	0.46	0.05	0.09	0.83	0.08
b.c h	65	25	10	1,100	$(Ca,Mg,Fe)CO_3$	0.68	0.26	0.07	–	–	–
b.c n	70	25	5	1,100	$(Ca,Mg,Fe)CO_3$	0.68	0.29	0.03	–	–	–
b.c o	60	35	5	1,100	$(Ca,Mg,Fe)CO_3$	0.60	0.35	0.04	–	–	–
b.c q	25	25	50	1,100	$(Ca,Mg,Fe)CO_3$	0.36	0.29	0.35	–	–	–
b.c s	25	0	75	1,100	$(Ca,Mg,Fe)CO_3$	0.57	0.01	0.42	–	–	–

Table 1 continued

Run	Starting material (wt%)			T	Run Products	Phase 1 (mol.%)			Phase 2 (mol.%)		
	Cc	Mgs	Sid	(°C)		Cc	Mgs	Sid	Cc	Mgs	Sid
b.c t	75	0	25	1,100	$(Ca, Fe)CO_3$	0.81	0.00	0.18	–	–	–
b.cAA	15	35	50	1,100	$(Ca,Mg,Fe)CO_3$	0.14	0.40	0.46	–	–	–
b.cAB	12	28	60	1,100	$(Ca,Mg,Fe)CO_3$	0.11	0.33	0.56	–	–	–
b.cAC	9	21	70	1,100	$Dol_{s.s.} + Mgs_{s.s}$	0.40	0.35	0.25	0.14	0.53	0.33
b.cAM	24.4	24.7	50.9	1,100	$Dol_{s.s.} + Mgs_{s.s}$	0.38	0.30	0.33	0.16	0.45	0.39
b.cAN	23.7	16	60.7	1,100	$(Ca,Mg,Fe)CO_3$	0.30	0.20	0.50	–	–	–

Cc, Mgs, Sid (wt%) define starting material bulk compositions expressed in weight %. Phase 1 and Phase 2 (mol.%), phase compositions of the run products expressed in mole %. *Cc* calcite, *Mgs* magnesite, *Sid* siderite. $Dol_{s.s.}$ = mineral with composition close to $Ca_{0.5}(Mg,Fe)_{0.5}CO_3$; $Mgs_{s.s.}$ mineral with composition close to the solid solution siderite-magnesite with <10 mol% $CaCO_3$ component

beam, the probe current was reduced to 3–6 nA and the spot size broadened to 20 μm where possible. The best compromise between count statistical error and volatilization was found when counting 40 s on peak and 20 s on background. Natural carbonate standards were used (calcite, magnesite, siderite and dolomite) and CO_2 was calculated by stoichiometry. Under these conditions, it was possible to obtain analytical totals of 100 ± 3 wt% including calculated CO_2, and only data meeting this threshold were considered.

Experimental results

Textural features of the experiments (Fig. 2) include the presence of triple junctions, homogenous phase compositions and well-crystallized starting materials, all of which influence attaining equilibrium during the experiments. At 900°C carbonates form 5–10 μm polyhedral grains, growing with temperature to 80–100 μm at 1,100°C. Magnetite was detected in all runs and is an inherent product of siderite oxidation. This oxidation

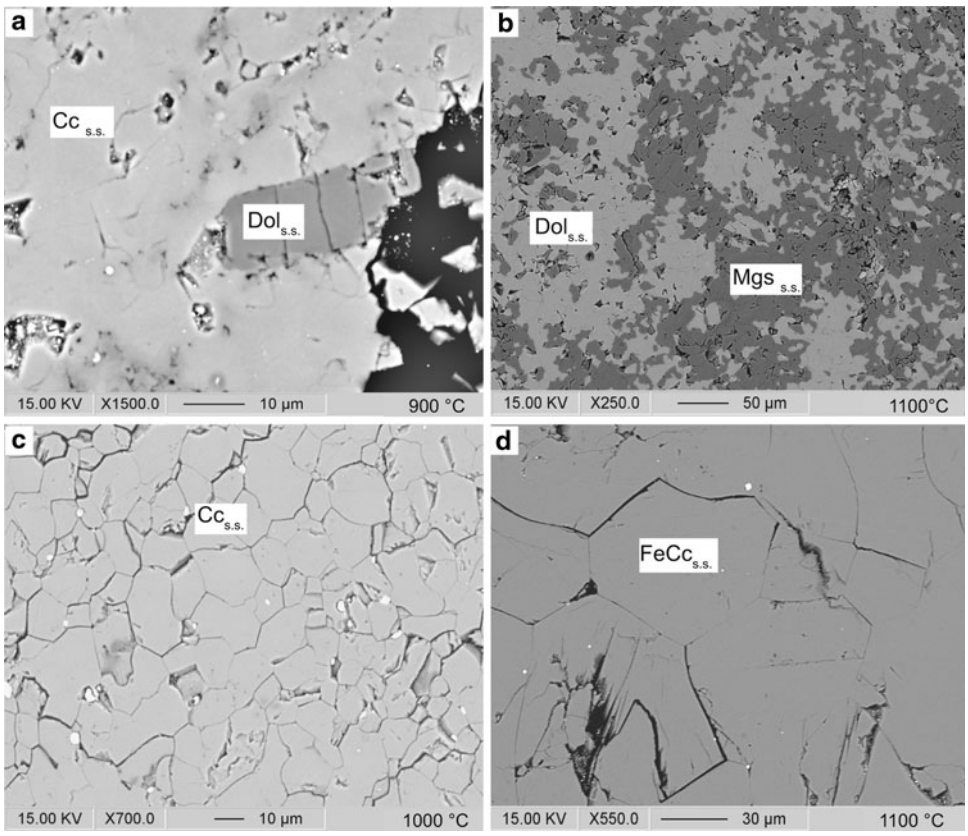

Fig. 2 BSE images showing textural features of experimental charges. **a** Coexistence of $Dol_{s.s}$ with $Cc_{s.s.}$ at 900°C, experiment *n* (Table 1). **b** $Dol_{s.s.}$ coexisting with $Mgs_{s.s.}$ at 1,100°C, experiment *g* **c** Single phase $Cc_{s.s.}$ synthesized at 1,000°C, experiment *x*. **d** Fe–$Cc_{s.s}$ showing grain growth of carbonates up to 80 μm at 1,100°C, experiment *t*. Magnetite has been detected in all experiments and is recognizable as white micron-size speckles in **a**, **c**, and **d**. $Cc_{s.s.}$ Mg–Fe Calcite solid solution; $Dol_{s.s.}$ solid solution near the join $CaMg(CO_3)_2$–$CaFe(CO_3)_2$; $Mgs_{s.s.}$ solid solution near the join $MgCO_3$–$FeCO_3$; $FeCc_{s.s.}$ $CaCO_3$–$CaFe(CO_3)_2$ solid solution

shifts the effective carbonate bulk compositions away from the $FeCO_3$ component, leading to some difficulties controlling carbonate compositions near the $FeCO_3$ corner.

The amount of magnetite in the run products increases both with Fe content in the bulk and with temperature. Experimental results are reported in Table 1 and plotted with a visual fit of the data outlining the solvi in Fig. 1d, f. Two miscibility gaps were observed at 900°C. The dolomite–calcite solvus closes at an X_{MgCO3} near 0.7 and the dolomite–magnesite solvus is continuous with the miscibility gap siderite–ankerite, the latter being slightly enriched in Ca with respect to its nominal composition. With increasing temperature, the two miscibility gaps become narrower until the calcite–dolomite solvus disappears between 1,000 and 1,100°C where, as already observed at lower pressure by Goldsmith and Heard (1961), solid solution between dolomite and calcite is complete (Fig. 3a). The miscibility gap between dolomite and magnesite is still present at 1,100°C, in agreement with the data of Irving and Wyllie (1975) at 3.0 GPa and with lower pressure data (Byrnes and Wyllie 1981). $Ca_{0.525}Fe_{0.475}CO_3$ coexists with siderite at 900°C and complete miscibility was observed along the join $CaCO_3$–$FeCO_3$ at 1,000°C, leading to the closure of the binary solvus between 900 and 1,000°C, 100°C higher than that predicted by Davidson et al. (1993) at 3.0 GPa (Fig. 3b). At 3.5 GPa, 1,100°C, $Ca_{0.25}Fe_{0.75}CO_3$ is not stable anymore at the fO_2 imposed by the experimental setup and breaks down according to

$$2Ca_{0.25}Fe_{0.75}CO_3 = Ca_{0.5}Fe_{0.5}CO_3 + C + 1/3Fe_3O_4 + 5/6O_2 \quad (1)$$

Thermodynamic modeling

Even though the experimental system has only three components, its thermodynamic modeling is not trivial. The formulation of the free energy of mixing has to evaluate not only non-ideal mixing, but also order/disorder phenomena. Pyroxene solid solutions which, as carbonates, are characterized by order–disorder mechanisms have, among others, been studied by Green et al. (2007) and Holland and Powell (1996). In their solid solution models, the system $CaMgSi_2O_6$–$NaAlSi_2O_6$ was described introducing an intermediate ordered component, i.e., omphacite ($Ca_{0.5}Na_{0.5}Mg_{0.5}Al_{0.5}Si_2O_6$), to determine the pyroxene solid solution ordering state. Mineral (diopside and jadeite) and ordered (omphacite) components define a new set of independent end members able to deal with ordering and unmixing phenomena. A symmetric formalism has then been successfully applied to the above new set of end members to calculate phase diagrams including omphacitic pyroxenes (Green et al. 2007).

Carbonates have features very similar to pyroxenes with the intermediate ordered compound dolomite, which generates two solvi: dolomite-calcite and dolomite-magnesite. As the two solvi are strongly asymmetric (Goldsmith and Heard 1961), the symmetric formalism cannot describe them. To model the binary system $CaCO_3$–$MgCO_3$, asymmetry has been accommodated using the van Laar macroscopic formalism (Holland and Powell 2003). In the van Laar formulation, the activity terms are expressed not only as a function of interaction energies, as in the symmetric formalism, but also as a function of empirical "size parameters", i.e., α_i. The size parameters are defined for each end member and their differences account for the asymmetry (Holland and Powell 2003).

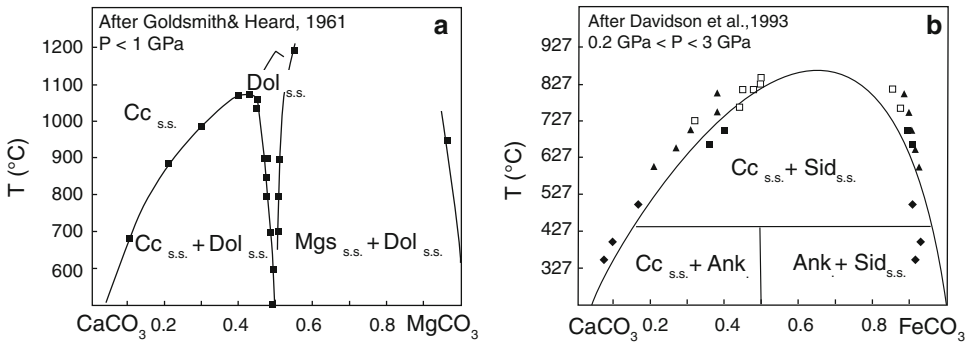

Fig. 3 **a** *T–X* diagram of the binary $CaCO_3$–$MgCO_3$ at pressures below 1.0 GPa, showing experimentally constrained phase relations after Goldsmith and Heard (1961). *Filled symbols* represent limits of the solvi as defined by the authors. **b** T-X diagram of the binary $CaCO_3$–$FeCO_3$ at pressures below 3.0 GPa, showing experimentally constrained phase relations after Davidson et al. (1993). *Square symbols* experiments by Davidson et al. (1993) at 3.0 GPa. Products from single phase starting materials (Ank) exsolving in two coexisting phases ($Cc_{s.s.}$–$Sid_{s.s.}$) shown as *filled squares*; those from two phases starting materials as *open squares*. *Filled triangles* experiments by Goldsmith et al. (1962) at 1.5 GPa, *filled diamonds* experiments by Rosenberg (1963) at ≤0.4 GPa. Solvus and phase stability fields are calculated with the model of Davidson et al. (1993), which predicts the stability of ordered ankerite up to ~450°C

We present a van Laar solid solution model for the ternary $CaCO_3$–$MgCO_3$–$FeCO_3$ based on five independent end members: three minerals and two ordered components. Thermodynamic properties for the mineral components calcite, magnesite and siderite are from the Holland and Powell database (Holland et al. 1998). The ordered components dolomite and "$Dol_{50}Ank_{50}$" are introduced to account for order/disorder in the ternary system. Interaction energies and size parameters have been determined calibrating activity–composition relations from the experimental data presented in Sects. 3 and 5.

Order–disorder

The structure of the ordered compound dolomite ($R\,\bar{3}$) consists of alternating octahedral layers of Ca^{2+} and Mg^{2+}, intercalated by planar CO_3^{2-} groups, defining M1 and M2 sites, which can preferentially host Ca or Mg respectively. With increasing temperature, Ca and Mg exchange between the two octahedral sites up to the critical temperature, where sites M1 and M2 become indistinguishable. The result is a disordered higher symmetry structure ($R\,\bar{3}c$). The degree of ordering can be quantified with the long-range order parameter s, defined as:

$$s = 2X_{Ca}^{M1} - 1 \quad (2)$$

where X_{Ca}^{M1} is the mole fraction of Ca hosted in the M1 site. The long-range order parameter s varies between 1 at low temperature, i.e., a completely ordered structure where every Ca^{2+} cation is hosted in the M1 site, to 0 above the critical temperature, i.e., completely disordered structure where Ca^{2+} cations are equally distributed over all octahedra.

Antao et al. (2004) investigated the state of order in dolomite as a function of temperature employing synchrotron in situ X-ray diffraction, thus observing the occurrence of the $R\,\bar{3} \Leftrightarrow R\,\bar{3}\,c$ phase transition at 1,466 K and 3.0 GPa.

Even though findings of Fe-enriched intermediate terms of the solid solution $CaMg(CO_3)_2$–$CaFe(CO_3)_2$ have been reported (Beran 1977), the pure end member ankerite ($CaFe(CO_3)_2$) has never been found in nature. Although calculated phase relations predict the stability of ordered $CaFe(CO_3)_2$ at $T \sim 450$°C (Davidson et al. 1993), attempts to synthesize this phase have yet failed. Structural variations of intermediate compounds along the join $CaMg(CO_3)_2$–$CaFe(CO_3)_2$ have been examined with single crystal X-ray diffraction, Mössbauer spectroscopy and transmission-electron microscopy (Reeder and Dollase 1989), showing that Fe substitutes Mg in the ordered structure up to a $X_{CaFe(CO3)2}$ of $\sim$70%.

Our thermodynamic model of the system $CaCO_3$–$MgCO_3$–$FeCO_3$ incorporates order–disorder phase transitions. Although order–disorder mechanisms in dolomite have been explored, long-range order processes remain poorly constrained for compositions other than dolomite.

Computed subsolidus phase relations: solid solution model

Along the join $CaCO_3$–$MgCO_3$, the state of order is defined by the partitioning of Ca and Mg between the sites M1 and M2 (Eq. 2), which become equivalent at high temperature. The degree of ordering is given by the internal equilibrium reaction

$$\frac{1}{2}\text{calcite} + \frac{1}{2}\text{magnesite} = \text{dolomite} \quad (3)$$

characterized by the enthalpy of ordering ΔH_R^{dol} (Holland and Powell 2003). Even though Holland and Powell (2003) preliminarily set the enthalpy of ordering of dolomite ΔH_R^{dol} to -13.5 kJ/mol, and Navrotsky and Capobianco (1987) calculated from calorimetric measurements the enthalpy of ordering to -5.74 kJ/mol, we set ΔH_R^{dol} to -1 kJ/mol. This latter value, along with other energetic parameters, predicts the disordering temperature of dolomite in accordance with the results of in situ experiments analyzed at a synchrotron in a parallel study (Franzolin et al. submitted). The effect of the enthalpy of ordering is best shown when calculating the dissociation reaction of fully ordered stoichiometric dolomite. Figure 4 shows the experiments by Harker and Tuttle (1955a) constraining this dissociation reaction into periclase + calcite + CO_2 and the calculated reaction positions (calculated employing Perplex_07 by Connolly (2005) and the 2002 update of the Holland and Powell database) for the various enthalpies of ordering. The Holland and Powell (HP'03) and Navrotsky and Capobianco (NC'87) enthalpies of ordering lead to an overestimation of the thermal stability of dolomite by more than 150 and 60°C, respectively; on the other hand, setting ΔH_R^{dol} to -1 kJ/mol leads to an underestimation of the stability of dolomite by about 40°C. Goldsmith (1980) has studied the same dolomite dissociation reaction at pressures higher than 1.5 GPa. With increasing pressure, the slope of the dolomite dissociation reaction has a turning point where dolomite becomes Ca-enriched, forming a solid solution with calcite as pure dolomite becomes unstable. Thus, calculating this reaction would include a departure from stoichiometric dolomite and thus a solid solution model and, consequently, for the evaluation of ΔH_R^{dol}, we limit ourselves to the low pressure data.

Introducing Fe into the system complicates the partitioning of Ca, Mg and Fe between the crystallographic sites. A new ordered compound is needed to describe order/disorder between Fe–Mg and Fe–Ca. Whereas the stability of ordered intermediate compounds along the join $CaMg(CO_3)_2$–$CaFe(CO_3)_2$ has been demonstrated, the stability of ordered stoichiometric ankerite $CaFe(CO_3)_2$ is

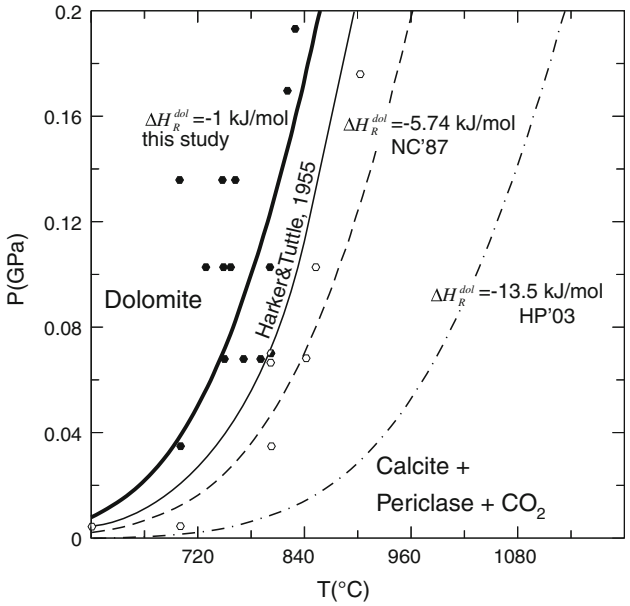

Fig. 4 Dissociation reaction of dolomite to calcite + periclase + CO_2 as experimentally determined by Harker and Tuttle (1955a); *filled symbols* represent dolomite stable, *open symbols* the association calcite + periclase + CO_2. Experiments are compared with calculated dolomite dissociation reaction based on three different enthalpies of ordering for dolomite: −13.5 kJ/mol, as proposed by Holland and Powell (2003); *dashed-point line* −5.74 kJ/mol as proposed by Navrotsky and Capobianco (1987); *dashed line* –1 kJ/mol, this study, *bold line*

not yet confirmed. Therefore, a new ordered compound is introduced and termed "$Dol_{50}Ank_{50}$"; it is the intermediate term of the join $CaMg(CO_3)_2$–$CaFe(CO_3)_2$ and defined by the internal equilibrium reaction

$$\frac{1}{2}\text{calcite} + \frac{1}{4}\text{magnesite} + \frac{1}{4}\text{siderite} = Dol_{50}Ank_{50} \qquad (4)$$

characterized by the enthalpy of ordering $\Delta H_R^{Dol_{50}Ank_{50}}$, set to −750 J/mol. The enthalpy of formation of dolomite increases with increasing Fe content (Navrotsky et al. 1999), and therefore the enthalpy of formation of $Dol_{50}Ank_{50}$ is higher than that of dolomite. Following the same criterion used for the enthalpy of ordering of dolomite, we set the enthalpy of ordering of $Dol_{50}Ank_{50}$ to −750 J/mol, because this value predicts the disordering temperature of $Ca_{0.5}Mg_{0.25}Fe_{0.25}CO_3$ in agreement with in situ experiments mentioned above (Franzolin et al. submitted).

To define Fe–Mg and Fe–Ca ordering processes, we assume that the new ordered compound $Dol_{50}Ank_{50}$ hosts Ca preferentially in the M1 sites and that the M2 sites is split into two different crystallographic sites: M2a and M2b, which host Fe and Mg, respectively. Although suitable crystallographic observations have not been yet targeted at a possible M2 site splitting in Fe-rich dolomite, the possibility of clustering or of Mg–Fe ordering between M2a and M2b sites cannot be excluded (Reeder and Dollase 1989). The ternary system $CaCO_3$–$MgCO_3$–$FeCO_3$, which allows ordering of Ca, Mg, and Fe over three crystallographic sites M1, M2a, M2b, is treated as a fictive system defined by the following five end members:

$$\begin{aligned}
&\text{calcite } (cc) = (Ca_{0.5}^{M1}Ca_{0.25}^{M2a}Ca_{0.25}^{M2b})CO_3\\
&\text{dolomite (dol)} = (Ca_{0.5}^{M1}Mg_{0.25}^{M2a}Mg_{0.25}^{M2b})CO_3\\
&\text{magnesite (mag)} = (Mg_{0.5}^{M1}Mg_{0.25}^{M2a}Mg_{0.25}^{M2b})CO_3\\
&\text{siderite (sid)} = (Fe_{0.5}^{M1}Fe_{0.25}^{M2a}Fe_{0.25}^{M2b})CO_3\\
&Dol_{50}Ank_{50}\ (D_{50}A_{50}) = (Ca_{0.5}^{M1}Fe_{0.25}^{M2a}Mg_{0.25}^{M2b})CO_3
\end{aligned}$$

The following order parameters can be defined:

$$\begin{aligned}
Q_1 &= (X_{Mg}^{M2b} - X_{Mg}^{M2a})\\
Q_2 &= (X_{Mg}^{M2b} - X_{Mg}^{M1})\\
V_1 &= (X_{Fe}^{M2a} - X_{Fe}^{M1})\\
V_2 &= (X_{Fe}^{M2a} - X_{Fe}^{M2b})
\end{aligned} \qquad (5)$$

As three of these four order parameters are equivalent (Q_1, V_1, V_2), only two order parameters are needed to describe cation speciation: Q (i.e., Q_2) and V (i.e., Q_1, V_1, V_2). Q and V can vary from completely ordered, i.e., equal to 1, to completely disordered, i.e., equal to 0, as summarized in Fig. 5. Internal equilibrium reactions (3) and (4) define the equilibrium state of order as a function of temperature and composition (Holland and Powell 1996). Two compositional parameters

$$\begin{aligned}
X &= \frac{1}{2}X_{Mg}^{M1} + \frac{1}{4}X_{Mg}^{M2a} + \frac{1}{4}X_{Mg}^{M2b}\\
J &= \frac{1}{2}X_{Fe}^{M1} + \frac{1}{4}X_{Fe}^{M2a} + \frac{1}{4}X_{Fe}^{M2b},
\end{aligned} \qquad (6)$$

are defined, where X and J are the magnesite and siderite mol-fractions, respectively. The site fractions in the partially ordered carbonates are then defined as follows:

$$\begin{aligned}
X_{Ca}^{M1} &= 1 - X - J + \frac{Q}{2}\\
X_{Mg}^{M1} &= X - \frac{Q}{2} + \frac{V}{4}\\
X_{Fe}^{M1} &= J - \frac{V}{4}\\
X_{Ca}^{M2a} &= 1 - X - J - \frac{Q}{2}\\
X_{Mg}^{M2a} &= X + \frac{Q}{2} - \frac{3}{4}V\\
X_{Fe}^{M2a} &= J + \frac{3}{4}V\\
X_{Ca}^{M2b} &= 1 - X - J - \frac{Q}{2}\\
X_{Mg}^{M2b} &= X + \frac{Q}{2} + \frac{V}{4}\\
X_{Fe}^{M2b} &= J - \frac{V}{4}
\end{aligned} \qquad (7)$$

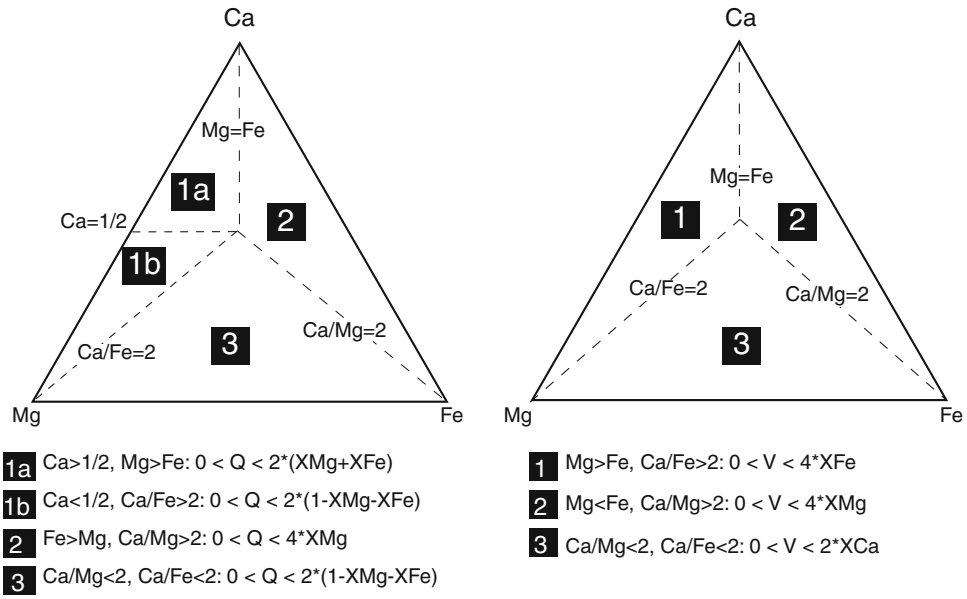

Fig. 5 State of ordering Q on the left, and V on the right, as function of composition. The chemical space has been divided in different regions where the order parameters vary from 0, completely disordered, to 1, completely ordered

and the proportions of the end members are given by

$$\begin{aligned} p_{cc} &= 1 - X - J - \frac{Q}{2} \\ p_{\mathrm{dol}} &= Q - V \\ p_{\mathrm{mag}} &= X - \frac{Q}{2} + \frac{V}{4} \\ p_{\mathrm{sid}} &= J - \frac{V}{4} \\ p_{\mathrm{ank}} &= V. \end{aligned} \tag{8}$$

In the van Laar macroscopic formalism the activity coefficient for an end member k in a phase with n independent end members is given by

$$RT \ln \gamma_k = -\sum_{i=1}^{n-1} \sum_{j>1}^{n} q_i q_j W_{ij}^*, \tag{9}$$

(Holland and Powell 2003), in which $q_i = 1 - \phi_i$ when $i = k$ and $q_i = -\phi_i$ when $i \neq k$, where ϕ_i is

$$\phi_i = \frac{p_i \alpha_i}{\sum_{j=1}^{n} p_j \alpha_j} \tag{10}$$

and

$$W_{ij}^* = W_{ij} \frac{2\alpha_k}{\alpha_i + \alpha_k}, \tag{11}$$

where p_i is the fraction of i in the phase k, as defined in Eqs. 8 and where the α parameters introduce asymmetry. If all α values are identical, Eq. 9 reduces to the symmetric formalism (Holland and Powell 2003). W_{ij} are the macroscopic interaction energies and W_{ij}^* are the "asymmetric interaction energies". As the system $CaCO_3$–$MgCO_3$–$FeCO_3$ shows a large degree of asymmetry, temperature dependence of the macroscopic interaction energies and of the α_i parameters is needed. A simple linear temperature dependence of the interaction energies W_{ij} can be written as

$$W_{ij} = W_{ij}^H - W_{ij}^S * T, \tag{12}$$

and likewise, for the size parameter α_i can be written as

$$\alpha_i = \alpha_i^H - \alpha_i^S * T, \tag{13}$$

with $W_{ij}^H$and α_i^Sgiving the necessary temperature correction of the interaction energies and size parameters, respectively. The published subsolidus phase diagrams indicate that the general topology, along the binary joins $CaCO_3$–$MgCO_3$ (Byrnes and Wyllie 1981; Goldsmith and Heard 1961; Graf and Goldsmith 1955, 1958; Harker and Tuttle 1955a, b; Irving and Wyllie 1975), $CaCO_3$–$FeCO_3$ (Davidson et al. 1993; Rosenberg 1963), and within the ternary phase diagram $CaCO_3$–$MgCO_3$–$FeCO_3$ (Goldsmith et al. 1962; Rosenberg 1967) does not change much with pressure, at least up to the breakdown of dolomite at 5–6 GPa. Therefore, an additional pressure dependency of these parameters is not justified by the data, leading to the assumption that the volume of mixing remains ideal.

Two groups of parameters must then be fit in our solid solution model: interaction energies and size parameters. For the binary joins these have been calculated with a Numerical Nonlinear Global Optimization method, utilizing the necessary condition that the chemical potentials of coexisting phases have to be equal at equilibrium. For the system $CaCO_3$–$MgCO_3$ our experimental results and the published data of Goldsmith and Heard (1961) and Harker and Tuttle (1955b) have been fitted together, while for the system $CaCO_3$–$FeCO_3$ our data have been fitted together with those of Davidson et al. (1993).

Table 2 Macroscopic interaction energies W_{ij} in J/mol, van Laar parameters and enthalpies of ordering in J/mol

	W_{ij}^H	W_{ij}^S
Energetic parameters		
Mag-Cc	28,000	0
Cc-Dol	11,200	0
Mag-Dol	14,000	0
Cc-Sid	20,503	0
$D_{50}A_{50}$-Sid	73,650	50
$D_{50}A_{50}$-Cc	12,730	10
Mag-Sid	10,000	0
Sid-Dol	51,190	30
$D_{50}A_{50}$-Dol	−5,000	0
$D_{50}A_{50}$-Mag	30,000	0
	α_i^H	α_i^S
van Laar parameters		
Cc	0.25	−0.000929
Dol	0.95	0
Sid	0.01	−0.000666
$D_{50}A_{50}$	0.929	0
Mag	1	0
Enthalpies of ordering		
$\Delta H_R^{D_{50}A_{50}}$	−750	
ΔH_R^{dol}	−1,000	

The size parameters α_i are dimensionless and normalized to unit value for magnesite. ΔH_R^{dol} = enthalpy of ordering for the reaction (3) in J/mol; $\Delta H_R^{Dol_{50}Ank_{50}}$ = enthalpy of ordering for reaction (4) in J/mol. *Dol* dolomite, *Mag* magnesite, *Cc* calcite; *Sid* siderite, $D_{50}A_{50}$ $Dol_{50}Ank_{50}$

The remaining interaction energies and size parameters necessary to describe phase relations in the ternary $CaCO_3$–$MgCO_3$–$FeCO_3$, have been refined on a trial and error base. The parameters have been adjusted to reproduce the experimentally determined phase diagrams, and to match phase relations determined by Goldsmith et al. (1962) and by Rosenberg (1967). The results are summarized in Table 2.

Computed subsolidus phase relations: results

Our fitted ternary carbonate solid solution model is then implemented into the solid solution data file of the program Perplex_07 (Connolly 2005) and $CaCO_3$–$MgCO_3$, $CaCO_3$–$FeCO_3$, and $CaCO_3$–$MgCO_3$–$FeCO_3$ phase relations then calculated (Figs. 6, 7) employing the 2002 update of the Holland and Powell database. Figure 6a shows the isobaric temperature-composition diagram calculated at 3.5 GPa for the system $CaCO_3$–$MgCO_3$. The calculation reproduces the miscibility gaps dolomite-calcite, closing at ~1,075°C, and dolomite-magnesite which is stable until cut by the solidus (Irving and Wyllie 1975). The calculated temperature-composition diagram for the system $CaCO_3$–$FeCO_3$ (Fig. 6b) predicts a broad solvus calcite-siderite, which closes at X_{FeCO3} ~0.7 and 980°C, while the critical temperature of the solvus proposed by Davidson et al. (1993) is ~850°C at X_{FeCO3} ~0.65.

Figure 7 shows calculated phase diagrams for the pressure–temperature conditions of this study (3.5 GPa and 900–1,100°C). At 900°C, our model reproduces the two

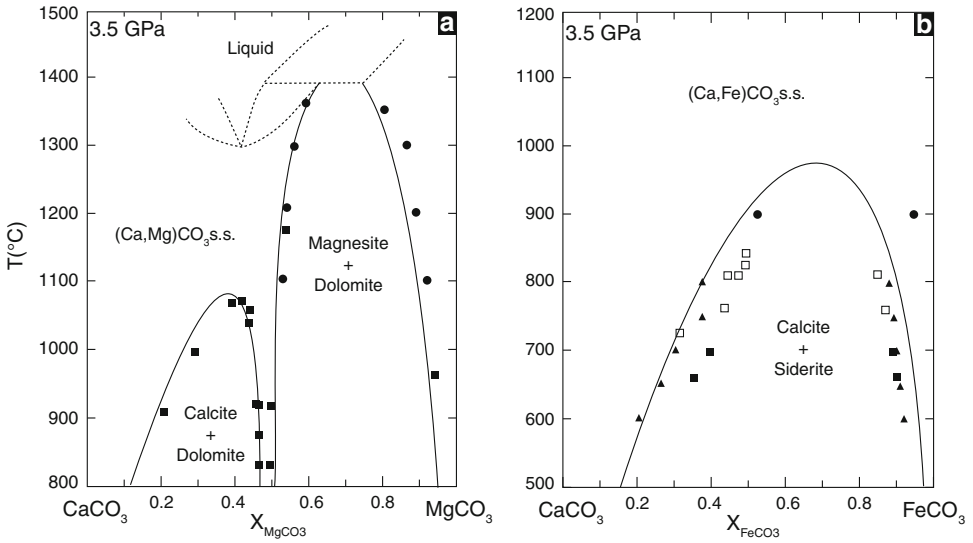

Fig. 6 Isobaric *T*–*X* section at 3.5 GPa of the join $CaCO_3$–$MgCO_3$ (**a**) and of $CaCO_3$–$FeCO_3$ (**b**) calculated from our solid solution model employing Perplex (Connolly 2005). *Dashed lines* in **a** represent the solidus and liquidus as determined by Irving and Wyllie (1975) at 3.0 GPa. For comparison experiments performed by Goldsmith and Heard (1961), $P < 1.0$ GPa, and Irving and Wyllie (1975) are plotted as *filled squares* and *circles*, respectively. *Square symbols* in **b** represent experiments performed by Davidson et al. (1993) at 3.0 GPa (compare to Fig. 3). *Filled triangles* experiments by Goldsmith et al. (1962) at 1.5 GPa; *filled circles* experiment performed in this study at 3.5 GPa

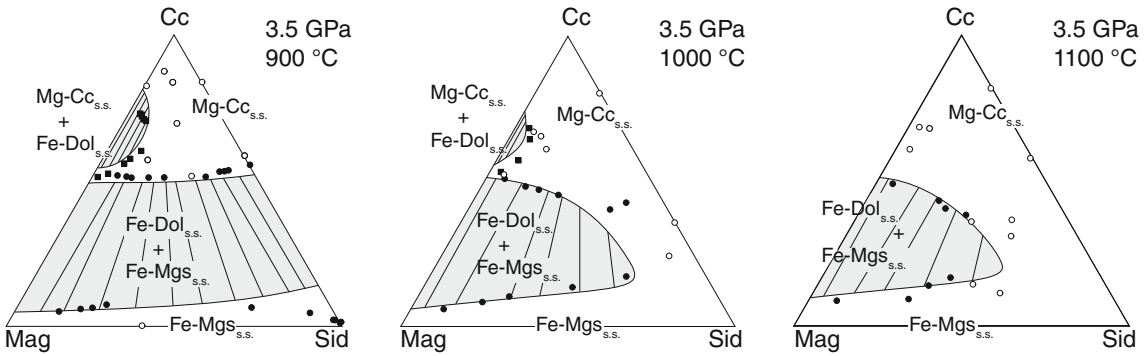

Fig. 7 Subsolidus relations in the system $CaCO_3$–$MgCO_3$–$FeCO_3$ at 3.5 GPa—900, 1,000 and 1,100°C as calculated from our solid solution model employing Perplex (Connolly 2005). The *gray areas* and *tie-lines* give 2-phase fields and coexisting phases. *Symbols* represent experiments performed in this study. *Open circles* indicate single phases, *filled circles* give coexisting phases (compare to Fig. 1)

experimentally observed miscibility gaps: the binary solvus dolomite–calcite, which closes at $X_{MgCO3} \sim 0.7$, in agreement with the experimental results, and the solvus dolomite–magnesite, which ranges to the Fe side of the ternary. The calculated tie-lines between the dolomite-ankerite s.s. and the magnesite-siderite s.s. slightly diverge from Fe dolomite. With increasing temperature the two calculated solvi shrink, and at 1,100°C the model predicts complete solid solution between dolomite and calcite, matching the experimental observations.

To show the reliability of our model in a wider pressure–temperature range, subsolidus phase relations have been calculated at P–T conditions outside our experimental coverage. The calculated phase diagram at 1.5 GPa, 600°C (Fig. 8a) is compared to the experiments of Goldsmith et al. (1962). The model is able to reproduce the features of the experimental phase relations, predicting a 3-phase field on the Fe-rich side of the diagram, which disappears at temperatures between 650 and 700°C. Goldsmith et al. (1962) do not specify compositions of coexisting phases; thus it is not possible to verify our calculated tie-lines. At higher temperature, i.e., at 1.5 GPa, 800°C (Fig. 8b), our model matches with good accuracy the experimental data of Goldsmith et al. (1962) along the solvus dolomite$_{s.s.}$–magnesite$_{s.s.}$, but does not fit the data defining the two-phase field dolomite$_{s.s.}$–calcite$_{s.s.}$. Goldsmith et al. (1962) predict the closure of the solvus at $X_{Fe} \sim 0.35$ (dashed line in Fig. 8b), but our calculated solvus closes at $X_{Fe} \sim 0.2$. Further support for a closure at low X_{Fe} stems from experiments performed in eclogitic system by Molina and Poli (2000) and Yaxley and Green (1994) (open squares and diamonds in Fig. 8b) which require complete solid solution between Fe dolomites with an $X_{Fe} \geq 0.15$ and calcite in the P–T range 1.2 GPa, 680°C to 3.0 GPa, 850°C.

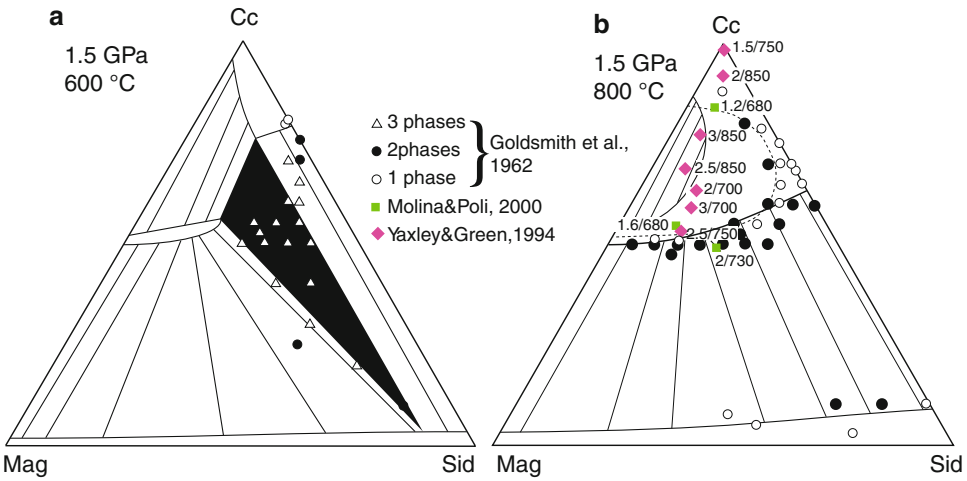

Fig. 8 Calculated subsolidus phase relations in the system $CaCO_3$–$MgCO_3$–$FeCO_3$ at 1.5 GPa, 600 (**a**) and 1.5 GPa, 800°C (**b**) employing our solid solution model. The *black triangle* gives the three phase field at 600°C (no such field results at 800°C). Experiments performed by Goldsmith et al. (1962) at the respective P–T conditions are reported for comparison in **a** and **b**; *open circles* single phase, *filled circles* two phase, *open triangle* three phase run products. The *dashed line* represents the solvus proposed by Goldsmith et al. (1962). Experimental single phase carbonates are represented by *green filled squares* (Molina and Poli 2000) and *pink filled diamonds* (Yaxley and Green 1994) in eclogitic systems, the experimental P–T conditions are indicated for each experiment as GPa/°C

These data are in discordance with the data of Goldsmith et al. (1962), and support a narrower Fe-bearing dolomite–calcite two-phase field at 800°C, as predicted by our model.

Assessment of the thermodynamic solution model

To further test the reliability of our model, pseudosections of experimentally studied anhydrous carbonated mafic bulk compositions have been calculated. The bulk compositions chosen are the SLEC1 composition from Dasgupta et al. (2004) and EC1 of Yaxley and Brey (2004), slightly modified to avoid the stability of trace amounts of olivine (Table 3). Subsolidus phase relations in the simplified system SiO_2–Al_2O_3–FeO–MgO–CaO–Na_2O–CO_2 ± TiO_2 have been calculated at pressures of 2–6 GPa and temperatures of 600–1,300°C (Fig. 9), while the solidi of both bulk compositions are from the original studies.

For SLEC1, our calculation shows the ubiquitous stability of clinopyroxene, ilmenite, and garnet. At low pressure, CO_2 vapor coexists with dolomite, which is the only carbon hosting phase near the solidus to pressures of 3 GPa (1,050°C). With increasing pressure, the dolomite + magnesite association appears, and magnesite is the final stable carbonate at higher pressures. Our calculated results are in good agreement with the subsolidus experiments performed by Dasgupta et al. (2004), who observed a shift of the carbon phase from CO_2 vapor at low pressure to dolomite and to dolomite + magnesite with increasing pressure. While the stability of the mineral association clinopyroxene + garnet + ilmenite + magnesite + dolomite has been experimentally observed only at 4.6 GPa, 1,010°C, calculated phase diagram predicts a broader stability field for this assemblage reaching toward lower pressures, with a small and decreasing weight fraction of magnesite with decreasing pressure (contour plots Fig. 9a).

The EC1 bulk has been simplified to SiO_2–Al_2O_3–FeO–MgO–CaO–Na_2O–CO_2 and the calculated pseudosection reproduces well the experimentally determined phase

Table 3 Carbonated eclogite bulk compositions used for pseudosections

	MSLEC1	MEC1	SLEC1	EC1
SiO_2	41.32	30.11	41.21	30.11
TiO_2	2.198	0	2.16	0
Al_2O_3	11.08	11.74	10.89	11.74
Cr_2O_3	0	0	0.09	0
FeO	13.06	10.05	12.83	10.05
MnO	0	0	0.12	0
MgO	12.27	12.42	12.87	12.44
CaO	13.32	19.42	13.09	19.41
Na_2O	1.659	0.87	1.63	0.87
K_2O	0	0	0.11	0
CO_2	5.089	15.39	5	15.38
Ca#	31.9	43.6	31.9	43.6
Mg#	64.1	68.8	64.1	68.8

MSLEC1 and MEC1 bulk composition are chemically simplified (Ti, Cr, Mn, K-free) compositions modified after SLEC1, the bulk composition of Dasgupta et al. (2004) and EC1 the bulk composition of Yaxley Brey (2004)

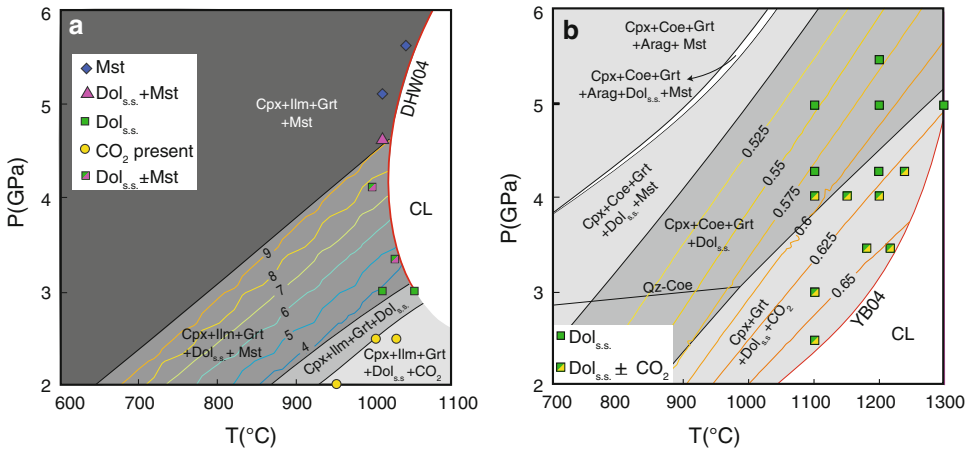

Fig. 9 Calculated pseudosections for carbonated eclogitic bulk compositions employing our carbonate solid solution model. **a** SLEC1 modified bulk composition (Table 3, MSLEC1). *Symbols* and *red bold line* (DHW04) are, respectively, experiments performed and carbonated eclogite solidus proposed by Dasgupta et al. 2004. Contours give calculated amounts of magnesite (wt%) in the assemblage. **b** EC1 modified bulk composition (Table 3, MEC1). *Red bold line* (YB04) is the carbonated eclogite solidus proposed by Yaxley and Brey (2004), *symbols* represent subsolidus experiments. Contours give calculated X_{Ca} of the dolomitic carbonate. **a**, **b** *Symbols* refer to the CO_2-bearing phase present in the experiments. *Yellow circles* CO_2 vapor; *green squares* dolomite; *green/yellow squares* dolomite + alleged CO_2 vapor; *pink triangle* dolomite + magnesite; *blue diamonds* magnesite; *green/pink squares* dolomite ± magnesite. Phase abbreviations are: *Cpx* clinopyroxene, *Ilm* ilmenite, *Grt* garnet, *Mst* magnesite, *Dol* dolomite, *CO_2* CO_2 vapor, *Qtz* quartz, *Coe* coesite, *CL* carbonatitic liquid

relationships. The composition of the dolomite solid solution is given as X_{Ca} isopleths (Fig. 9b): X_{Ca} increasing with temperature and decreasing with increasing pressure in accordance with the experiments. At 5 GPa and 900°C the calculated pseudosection predicts the breakdown of dolomite into aragonite + magnesite. Both, the SLEC1 and EC1 bulk compositions have comparable Mg#, but EC1 has a much higher Ca# which stabilizes dolomite solid solution over a broad P–T field.

Our solid solution model predicts correctly the subsolidus carbonate phases which are at the origin of the significantly higher carbonate melting temperatures of EC1 compared with SLEC1. Although thermodynamic carbonatite melt models are yet not available, our ternary solid solution model is a first step in predicting the subsolidus phase relations of eclogitic subducted carbonated materials and thus in predicting deep carbon recycling.

Concluding remarks

In this study we present experiments performed in the system $CaCO_3$–$MgCO_3$–$FeCO_3$ at 3.5 GPa, which allow depicting the ternary phase diagram at high pressure. Merging all experimental and previously published data, we develop a new solid solution model for Ca–Mg–Fe carbonates. The new solid solution model is able to describe order/disorder introducing "ordered end members", i.e., dolomite and $Dol_{50}Ank_{50}$. As experimental data show, the system $CaCO_3$–$MgCO_3$–$FeCO_3$ is characterized by asymmetric miscibility gaps, and the van Laar formalism has been introduced to deal with asymmetric non-ideal mixing. The thermodynamic model for ternary carbonates is reliable over a wide range of pressure–temperature conditions with an absolute minimum of fitted parameters. The model is available in the *perplex solut.dat* formats at www.perplex.ethz.ch, and is suitable to pressures of the breakdown of dolomite to aragonite + magnesite at ~6 GPa, and at least to temperatures of the ternary carbonate minimum melting, probably lying between 1,200 and 1,300°C.

Acknowledgments We are thankful to M.J. Caddick, D Grassi, H. Alistair, J.A.D. Connolly, A. Galli for discussions improving the manuscript. Thanks to U. Mann for technical support in the laboratory, to U. Graber and B. Zürcher for mechanical support. Rajdeep Dasgupta and an anonymous reviewer are thanked for helpful comments and suggestions. This work was funded by the European Commission through the Marie Curie Research training Network "c2c", Contract No. MRTN-CT-2006-035957.

References

Anovitz LM, Essene EJ (1987) Phase-equilibria in the system $CaCO_3$–$MgCO_3$–$FeCO_3$. J Petrol 28(2):389–414

Antao SM, Mulder WH, Hassan I, Crichton WA, Parise JB (2004) Cation disorder in dolomite, $CaMg(CO_3)(2)$, and its influence on the aragonite plus magnesite <=> dolomite reaction boundary. Am Mineral 89(7):1142–1147

Beran A (1977) Fissure ankerite from Steirische-Erzberg, possible utilization as geothermometer. Miner Depos 12:90–95

Biellmann C, Gillet P, Guyot F, Peyronneau J, Reynard B (1993) Experimental-evidence for carbonate stability in the Earths lower mantle. Earth Planet Sci Lett 118(1-4):31–41

Brey GP, Bulatov VK, Girnis AV, Lahaye Y (2008) Experimental melting of carbonated peridotite at 610 GPa. J Petrol 49(4):797–821

Buob A, Luth RW, Schmidt MW, Ulmer P (2006) Experiments on $CaCO_3$–$MgCO_3$ solid solutions at high pressure and temperature. Am Mineral 91(2–3):435–440

Burton BP (1987) Theoretical-analysis of cation ordering in binary rhombohedral carbonate systems. Am Mineral 72(3–4):329–336

Burton B, Kikuchi R (1984) Thermodynamic analysis of the system $CaCO_3$–$MgCO_3$ in the tetrahedron approximation of the cluster variation method. Am Mineral 69(1–2):165–175

Byrnes AP, Wyllie PJ (1981) Subsolidus and melting relations for the join $CaCO_3$–$MgCO_3$ at 10-Kbar. Geochim Cosmochim Acta 45(3):321–328

Capobianco C, Burton BP, Davidson PM, Navrotsky A (1987) Structural and calorimetric studies of order–disorder in $CdMg(CO_3)_2$. J Solid State Chem 71(1):214–223

Connolly JAD (2005) Computation of phase equilibria by linear programming: a tool for geodynamic modeling and its application to subduction zone decarbonation. Earth Planet Sci Lett 236(1–2):524–541

Dasgupta R, Hirschmann MM (2006) Melting in the Earth's deep upper mantle caused by carbon dioxide. Nature 440(7084):659–662

Dasgupta R, Hirschmann MM (2007) Effect of variable carbonate concentration on the solidus of mantle peridotite. Am Mineral 92(2–3):370–379

Dasgupta R, Hirschmann MM, Withers AC (2004) Deep global cycling of carbon constrained by the solidus of anhydrous, carbonated eclogite under upper mantle conditions. Earth Planet Sci Lett 227(1–2):73–85

Dasgupta R, Hirschmann MM, Dellas N (2005) The effect of bulk composition on the solidus of carbonated eclogite from partial melting experiments at 3 GPa. Contrib Mineral Petrol 149(3):288–305

Dasgupta R, Hirschmann MM, Smith ND (2007) Partial melting experiments of peridotite CO_2 at 3 GPa and genesis of alkalic ocean island basalts. J Petrol 48(11):2093–2124

Davidson PM (1994) Ternary iron, magnesium, calcium carbonates: a thermodynamic model for dolomite as an ordered derivative of calcite-structure solutions. Am Mineral 79(3–4):332–339

Davidson PM, Symmes GH, Cohen BA, Reeder RJ, Lindsley DH (1993) Synthesis of the new compound $CaFe(CO_3)_2$ and experimental constraints on the (Ca, Fe)CO_3 join. Geochim Cosmochim Acta 57(23–24):5105–5109

Domanik KJ, Holloway JR (2000) Experimental synthesis and phase relations of phengitic muscovite from 6.5 to 11 GPa in a calcareous metapelite from the Dabie Mountains, China. Lithos 52(1–4):51–77

Falloon TJ, Green DH (1989) The solidus of carbonated, fertile peridotite. Earth Planet Sci Lett 94(3–4):364–370

French BM (1971) Stability relations of siderite ($FeCO_3$) in system Fe–C–O. Am J Sci 271(1):37–78

Gillet P (1993) Stability of magnesite ($MgCO_3$) at mantle pressure and temperature conditions: a Raman-spectroscopic study. Am Mineral 78(11–12):1328–1331

Goldsmith JR (1980) Thermal stability of dolomite at high temperatures and pressures. J Geophys Res 85(NB12):6949–6954

Goldsmith JR, Heard HC (1961) Subsolidus phase relations in the system $CaCO_3$–$MgCO_3$. J Geol 69(1):45–74

Goldsmith JR, Graf DL, Witters J, Northrop DA (1962) Studies in the system $CaCO_3$–$MgCO_3$–$FeCO_3$.1. Phase relations.2. A method for major-element spectrochemical analysis.3. Compositions of some Ferroan dolomites. J Geol 70(6):659–688

Graf DL, Goldsmith JR (1955) Dolomite-magnesian calcite relations at elevated temperature and CO_2 pressures. Geochim Cosmochim Acta 7(3–4):109–128

Graf DL, Goldsmith JR (1958) The solid solubility of $MgCO_3$ in $CaCO_3$: a revision. Geochim Cosmochim Acta 13(2–3):218–219

Green E, Holland T, Powell R (2007) An order-disorder model for omphacitic pyroxenes in the system jadeite-diopside-hedenbergite-acmite, with applications to eclogitic rocks. Am Mineral 92(7):1181–1189

Hammouda T (2003) High-pressure melting of carbonated eclogite and experimental constraints on carbon recycling and storage in the mantle. Earth Planet Sci Lett 214(1–2):357–368

Harker RI, Tuttle OF (1955a) Studies in the system CaO–MgO–CO_2 1. The thermal dissociation of calcite, dolomite and magnesite. Am J Sci 253(4):209–224

Harker RI, Tuttle OF (1955b) Studies in the system CaO–MgO–CO_2 2. Limits of solid solution along the binary join $CaCO_3$–$MgCO_3$. Am J Sci 253(5):274–282

Holland T, Powell R (1996) Thermodynamics of order-disorder in minerals 2. Symmetric formalism applied to solid solutions. Am Mineral 81(11–12):1425–1437

Holland T, Powell R (2003) Activity–composition relations for phases in petrological calculations: an asymmetric multicomponent formulation. Contrib Mineral Petrol 145(4):492–501

Holland T, Baker J, Powell R (1998) Mixing properties and activity–composition relationships of chlorites in the system MgO–FeO–Al_2O_3–SiO_2–H_2O. Eur J Mineral 10(3):395–406

Irving AJ, Wyllie PJ (1975) Subsolidus and melting relationships for calcite, magnesite and join $CaCO_3$–$MgCO_3$ to 36 Kb. Geochim Cosmochim Acta 39(1):35–53

Isshiki M, Irifune T, Hirose K, Ono S, Ohishi Y, Watanuki T, Nishibori E, Takata M, Sakata M (2004) Stability of magnesite and its high-pressure form in the lowermost mantle. Nature 427(6969):60–63

Kerrick DM, Connolly JAD (2001) Metamorphic devolatilization of subducted oceanic metabasalts: implications for seismicity, arc magmatism and volatile recycling. Earth Planet Sci Lett 189(1–2):19–29

Korsakov AV, Hermann J (2006) Silicate and carbonate melt inclusions associated with diamonds in deeply subducted carbonate rocks. Earth Planet Sci Lett 241(1–2):104–118

Kraft S, Knittle E, Williams Q (1991) Carbonate stability in the Earths mantle: a vibrational spectroscopic study of aragonite and dolomite at high-pressures and temperatures. J Geophys Res 96(B11):17997–18009

Logvinova AM, Wirth R, Sobolev NV (2008) Nanometre-sized mineral and fluid inclusions in cloudy Siberian diamonds: new insights on diamond formation. Eur J Mineral 20(3):317–331

Luth RW (2001) Experimental determination of the reaction aragonite plus magnesite = dolomite at 5 to 9 GPa. Contrib Mineral Petrol 141(2):222–232

Martinez I, Zhang JZ, Reeder RJ (1996) In situ X-ray diffraction of aragonite and dolomite at high pressure and high temperature: evidence for dolomite breakdown to aragonite and magnesite. Am Mineral 81(5–6):611–624

Mcswiggen PL (1993a) Alternative solution model for the ternary carbonate system $CaCO_3$–$MgCO_3$–$FeCO_3$ 2. Calibration of a combined ordering model and mixing model. Phys Chem Miner 20(1):42–55

Mcswiggen PL (1993b) Alternative solution model for the ternary carbonate system $CaCO_3$–$MgCO_3FeCO_3$ 1 A ternary Braggwilliams ordering model. Phys Chem Miner 20(1):33–41

Molina JF, Poli S (2000) Carbonate stability and fluid composition in subducted oceanic crust: an experimental study on H_2O–CO_2–bearing basalts. Earth Planet Sci Lett 176(3–4):295–310

Mukherjee BK, Sachan HK, Ogasawara Y, Muko A, Yoshioka N (2003) Carbonate-bearing UHPM rocks from the Tso-Morari region, Ladakh, India: petrological implications. Int Geol Rev 45(1):49–69

Navrotsky A, Capobianco C (1987) Enthalpies of formation of dolomite and of magnesian calcites. Am Mineral 72(7–8):782–787

Navrotsky A, Dooley D, Reeder R, Brady P (1999) Calorimetric studies of the energetics of order–disorder in the system $Mg_{1-x}Fe_xCa(CO_3)_2$. Am Mineral 84(10):1622–1626

Ono S, Kikegawa T, Ohishi Y (2007) High-pressure transition of $CaCO_3$. Am Mineral 92(7):1246–1249

Philipp RW (1998) Phasenbeziehungen im system MgO–H_2O–CO_2–NaCl. Dissertation. ETH, Zurich

Poli S, Franzolin E, Fumagalli P, Crottini A (2009) The transport of carbon and hydrogen in subducted oceanic crust: an experimental study to 5 GPa. Earth Planet Sci Let 278(3-4):350–360

Reeder RJ, Dollase WA (1989) Structural variation in the dolomite-ankerite solid-solution series: an X-Ray, Mossbauer, and Tem Study. Am Mineral 74(9–10):1159–1167

Rosenberg PE (1963) Subsolidus relations in system $CaCO_3$–$FeCO_3$. Am J Sci 261(7):683–689

Rosenberg PE (1967) Subsolidus relations in system $CaCO_3$–$MgCO_3$–$FeCO_3$ between 350° and 550°C. Am Mineral 52(5–6):787–796

Sato K, Katsura T (2001) Experimental investigation on dolomite dissociation into aragonite plus magnesite up to 8.5 GPa. Earth Planet Sci Lett 184(2):529–534

Shirasaka M, Takahashi E, Nishihara Y, Matsukage K, Kikegawa T (2002) In situ X-ray observation of the reaction dolomite = aragonite plus magnesite at 900–1300 K. Am Mineral 87(7):922–930

Staudigel H (2003) Hydrothermal alteration processes in the Oceanic crust. In: Holland H, Turekian K (eds), vol 3. pp 511–537

Thomsen TB, Schmidt MW (2008a) The biotite to phengite reaction and mica-dominated melting in fluid carbonate-saturated pelites at high pressures. J Petrol 49(10):1889–1914

Thomsen TB, Schmidt MW (2008b) Melting of carbonated pelites at 2.5–5.0 GPa, silicate-carbonatite liquid immiscibility, and potassium-carbon metasomatism of the mantle. Earth Planet Sci Lett 267(1–2):17–31

van Roermund HLM, Carswell DA, Drury MR, Heijboer TC (2002) Microdiamonds in a megacrystic garnet websterite pod from Bardane on the island of Fjortoft, western Norway: evidence for diamond formation in mantle rocks during deep continental subduction. Geology 30(11):959–962

Vinograd VL, Winkler B, Putnis A, Gale JD, Sluiter MHF (2006) Static lattice energy calculations of mixing and ordering enthalpy in binary carbonate solid solutions. Chem Geol 225(3–4):304–313

Vinograd VL, Burton BP, Gale JD, Allan NL, Winkler B (2007) Activity–composition relations in the system $CaCO_3$–$MgCO_3$ predicted from static structure energy calculations and Monte Carlo simulations. Geochim Cosmochim Acta 71(4):974–983

Wang A, Pasteris JD, Meyer HOA, DeleDuboi ML (1996) Magnesite-bearing inclusion assemblage in natural diamond. Earth Planet Sci Lett 141(1–4):293–306

Yaxley GM, Green DH (1994) Experimental demonstration of refractory carbonate-bearing eclogite and siliceous melt in the subduction regime. Earth Planet Sci Lett 128:313–325

Yaxley GM, Brey GP (2004) Phase relations of carbonate-bearing eclogite assemblages from 2.5 to 5.5 GPa: implications for petrogenesis of carbonatites. Contrib Mineral Petrol 146(5):606–619